A Mechanism-Based Combination Therapy Reduces Local Tumor Growth and Metastasis in an Orthotopic Model of Prostate Cancer

Boleslav Kosharskyy,[1] Nicolas Solban,[2] Sung K. Chang,[2] Imran Rizvi,[2] Yuchiao Chang,[2] and Tayyaba Hasan[2]

[1]Department of Anesthesiology, Mount Sinai Hospital, New York, New York and [2]Wellman Center for Photomedicine, Massachusetts General Hospital, Harvard Medical School, Boston, Massachusetts

Abstract

Therapy-induced stimulation of angiogenic molecules can promote tumor angiogenesis leading to enhanced tumor growth and cancer metastasis. Several standard and emerging therapies, such as radiation and photodynamic therapy (PDT), can induce angiogenic molecules, thus limiting their effectiveness. PDT is approved for the treatment of several cancers; however, its induction of vascular endothelial growth factor (VEGF) creates conditions favorable to enhanced tumor growth and metastasis, therefore mitigating its cytotoxic and antivascular effects. This is the first report showing that subcurative PDT in an orthotopic model of prostate cancer (LNCaP) increases not only VEGF secretion (2.1-fold) but also the fraction of animals with lymph node metastases. PDT followed by administration of an antiangiogenic agent, TNP-470, abolished this increase and reduced local tumor growth. On the other hand, administration of TNP-470 before PDT was less effective at local tumor control. In addition, animals in all groups, except in the PDT + TNP-470 group, had a weight loss of >3 g at the time of sacrifice; the weight of the animals in the PDT + TNP-470 group did not change. The significant reduction ($P < 0.05$) in tumor weight and volume observed between the PDT + TNP-470 group and the control group suggests that the combination of PDT and antiangiogenic treatment administered in the appropriate sequence was not only more effective at controlling local tumor growth and metastases but also reduced disease-related toxicities. Such molecular response-based combinations merit further investigations as they enhance both monotherapies and lead to improved treatment outcomes. (Cancer Res 2006; 66(22): 10953-8)

Introduction

Photodynamic therapy (PDT) consists of the systemic or local administration of a photosensitizer and its subsequent activation by visible light. In the presence of oxygen, activated photosensitizer can generate reactive oxygen species that are toxic to the tumor (1, 2). With the use of modern fiber optic systems and various types of endoscopy, light can now be targeted accurately to almost any part of the body, significantly increasing the number of PDT applications. PDT is approved as a first line treatment for age-related macular degeneration and for a variety of cancers (3). Porfimer sodium (Photofrin) is approved for use in advanced and early-stage lung cancers, superficial gastric cancer, esophageal adenocarcinoma, cervical cancer, bladder cancer, and Barrett's esophagus. Temoporfin, another photosensitizer, is approved in Europe for the palliative treatment of head and neck cancers. Topically applied photosensitizers are also approved for the treatment of actinic keratosis and basal cell carcinomas. PDT is also under investigation for the treatment of other neoplasias (2, 4), and the feasibility of using PDT for the treatment of localized recurrent prostate cancer has also been shown previously and may be a viable treatment option (5–7).

As PDT becomes more of a mainstream treatment option for early cancers, it is important to understand the factors that might mitigate its tumoricidal effect. We have reported previously an increase in the number of lung metastases following subcurative BPD (benzoporphyrin derivative)-PDT in a highly aggressive prostate cancer model (8). More recently, we and others have reported an increase in the synthesis and secretion of vascular endothelial growth factor (VEGF) following subcurative PDT (9–11). The molecular responses of PDT-treated tumors have been investigated to design novel mechanism-based treatment regimens to improve PDT efficacy and long-term patient health. Along these lines, Ferrario et al. (10) have shown an increase in hypoxia-inducible factor-1α (HIF-1α) following Photofrin-mediated PDT of a s.c. BA mouse mammary carcinoma and an increase in cyclooxygenase-2 (COX-2) following PDT (11) leading to an increase in VEGF. On the other hand, we showed recently that, in the LNCaP prostate cancer cell line, the VEGF increase following BPD-PDT occurred independently of HIF-1α and COX-2 but was induced by the p38 mitogen-activated protein kinase pathway (9). Taken together, these results suggest that tumor responses to PDT at the molecular level are not generic but probably depend on the tumor type, the site of implantation, and the photosensitizer used for treatment. These observations prompted the current study, which to our knowledge is the first report of the effect of subcurative PDT not only on VEGF induction but also on lymph node metastasis in an orthotopic model of prostate cancer using the LNCaP cells, a human cell line.

In addition to the well-documented increase in angiogenesis (12, 13) and in VEGF (9, 10) following subcurative PDT, many other molecules, such as interleukin-8, fibroblast growth factor-2, epidermal growth factor, and platelet-derived growth factor, can also promote angiogenesis (reviewed in ref. 14), and some of these cytokines are up-regulated following PDT *in vitro* (15, 16). In the current study, we decided to use TNP-470, a molecule that inhibits the action of VEGF (angiogenesis), instead of a molecule specific to VEGF. TNP-470 is a synthetic analogue of fumagillin, which

Note: B. Kosharskyy and N. Solban contributed equally to this work.

Requests for reprints: Tayyaba Hasan, Wellman Center for Photomedicine, Massachusetts General Hospital, 40 Blossom Street, Boston, MA 02114. Phone: 617-726-6996; Fax: 617-726-8566; E-mail: thasan@partners.org.

doi:10.1158/0008-5472.CAN-06-1793

strongly inhibits vascular endothelial cell proliferation and migration (17) by blocking methionyl aminopeptidase-2 (MetAP2). Furthermore, TNP-470 is under phase 1 clinical trial for the treatment of prostate cancer (18–20). We hypothesized that the combination of TNP-470 and PDT may improve local control and reduce metastasis.

Disease processes in cancer are complex, and single treatment modalities may not be totally effective. However, rationally designed, mechanism-based combination therapies may have greater chance of success. The results presented in this study show that an understanding of factors that limit PDT efficacy could lead to novel combination therapies that improve treatment outcome not only in terms of local tumor control but also by inhibiting metastasis and by reducing disease related toxicities.

Materials and Methods

Cell culture and reagents. LNCaP, human prostate carcinoma cells, were obtained from American Type Culture Collection. Monolayer cultures were incubated in RPMI 1640 (Mediatech, Herndon, VA) supplemented with 10% FCS (Invitrogen, Carlsbad, CA), 100 units/mL penicillin, 100 μg/mL streptomycin (Mediatech), and 10 mmol/L HEPES. Liposomal BPD (0.25 mg/kg body weight) and TNP-470 (30 mg/kg body weight) were used in all *in vivo* studies. Liposomal BPD was donated by QLT, Inc. (Vancouver, British Columbia, Canada), and the TNP-470 was a gift of Dr. Folkman (Vascular Biology Program, Children's Hospital Boston, Boston, MA).

Tumor implantation. Experiments were carried out on 6-week-old male severe combined immunodeficient (SCID) mice weighing ~25 g (Cox Breeding Laboratories, Cambridge, MA). Animals were anesthetized with a 7:1 mixture of ketamine/xylazine. A 2-cm longitudinal incision from the pubic bone in a cranial direction exposed the prostate after the bladder was retracted cranially. Next, 3×10^6 LNCaP cells in 50% Matrigel (BD Biosciences, San Diego, CA) were injected into the stroma of the prostate ventral lobe (total injection volume of 0.1 mL). The incision was closed with 2-0 sutures. Three weeks following injection, a 0.1 to 0.2 cm^3 tumor develops.

PDT. TNP-470 was injected on days 13, 15, 17, and 19 (for the TNP-470 group and for the TNP-470 + PDT group) or on days 23, 25, 27, and 29 (for the PDT + TNP-470 group) after the orthotopic implantation of the tumor cells, whereas PDT was done on day 21 after the implantation of cells. For PDT, liposomal BPD was injected into the tail vein of mice 1 hour before irradiation. Before irradiation, a laparotomy was done and the prostate tumor was exposed. The tumor was irradiated at a fluence of 100 J/cm^2 using a 690-nm diode laser (High Power Devices, Inc., North Brunswick, NJ). The incision was then closed. For ELISA, the animals were euthanized and the tumors were collected 24 hours after treatment (day 22). To evaluate the treatment response, the animals were euthanized and the tumors were collected 40 days after implantation.

ELISA. For VEGF measurements, proteins were extracted from orthotopic prostate tumors 24 hours following PDT treatment. Briefly, frozen tumors were pulverized to powder in a tissue homogenizer and thawed in 1 mL/mg lysis buffer containing protease inhibitors (1% PBS, 1% NP40, 0.5% sodium deoxycholate, 0.1% SDS, 10 mg/mL phenylmethylsulfonyl fluoride, 100 mmol/L sodium orthovanadate, protease inhibitors). The protein concentration was determined using a standard Lowry method. A human VEGF DuoSet ELISA Development System (R&D Systems, Minneapolis, MN) was used to quantify human VEGF levels. Results were normalized to proteins.

Treatment response. Forty days after implantation, the animals were sacrificed by carbon dioxide asphyxiation. Pelvic lymph nodes, along with the entire prostate tissue, liver, and lungs, were removed. Prostate tissue was weighed. Lymph nodes and liver were fixed with 10% formalin for histologic examination and identification of metastases. The lungs had Bouin's solution injected intratracheally and were kept immersed for 4 days before the metastatic colonies were counted.

Analysis of micrometastases. Mice were sacrificed by CO_2 inhalation. The lymph nodes were removed and fixed in 10% formalin. The formalin-fixed lymph nodes were embedded in paraffin and serial sections (5-μm thick) were cut throughout each entire lymph node. Sections were stained with H&E using standard procedures. H&E-stained lymph node sections were analyzed for tumor cells microscopically under ×40 and ×100 magnifications. Tumor nodules were identified as densely packed large mitotic cells.

***In vivo* imaging.** The fluorescently labeled molecule Alexa Fluor 647-bovine serum albumin (BSA; Invitrogen) was injected into the tail vein (0.125 mg) of anesthetized mice. Immediately following injection, a laparotomy exposed the prostate tumor, which was imaged using the Maestro *in vivo* imaging system (Cambridge Research and Instrumentation, Inc., Woburn, MA). Twenty-one days after orthotopic implantation, the tumors were imaged immediately before PDT, 24 hours (day 22) and 96 hours (day 24) following treatment; images were acquired every minute for the first 10 minutes and every 2 minutes for the final 10 minutes. To analyze the change in fluorescence with time, the tumor region in each image was divided into three nonoverlapping areas. The three areas selected for each tumor were kept constant throughout the images acquired at different time points. Average fluorescence intensity per pixel was calculated from each of these three areas.

Statistical evaluation. Data were represented as the mean ± SE of three independent experiments. A comparison of VEGF production by ELISA between PDT and no treatment or BPD only was calculated by unpaired Student's t test, and a mixed-effects model for repeated measures analysis was used for *in vivo* measurement comparisons. $P < 0.05$ was considered statistically significant.

Results

Subcurative PDT increases VEGF. LNCaP cells in 50% Matrigel were injected in the prostate of male SCID mice. This orthotopic prostate cancer model has been well established in the laboratory, and 3 weeks following injection, a 0.1 to 0.2 cm^3 tumor develops in ~90% of animals injected. One hour before PDT, 0.25 mg/kg liposomal BPD was injected i.v. Laser irradiation was done after a laparatomy exposed the tumor at a fluence of 100 J/cm^2. The following day, the animals were sacrificed, the tumors were collected, and VEGF levels were quantified by ELISA (Fig. 1). PDT induced a 2.1-fold increase in VEGF ($P < 0.05$) when compared with no treatment or to BPD only. In previous studies, under identical conditions, we did not observe any effect of light alone treatment (8).[3] For this reasons, we did not include a light only control.

Transient vascular shutdown following PDT. We have shown previously that 1 hour following liposomal BPD injection, the photosensitizer is localized both in the vasculature and in the tumor (9). Furthermore, because PDT with vascular photosensitizers induces vascular shutdown, we decided to evaluate the functionality of the tumor vasculature following PDT. The fluorophore, Alexa Fluor 647-BSA, was injected i.v. immediately before imaging the prostate tumor. Fluorescence in the untreated animal steadily increases over time (Fig. 2*A, bottom*), suggesting that the fluorophore diffuses out of the tumor vasculature. Immediately after PDT (data not shown) and 24 hours following treatment, no fluorescence is detected in the tumor, suggesting vascular shutdown (Fig. 2*B, bottom*). However, 96 hours following treatment, fluorescence can be detected in the tumor (Fig. 2*C, bottom*), indicative of functional vasculature. Interestingly, fluorescence levels do not increase as rapidly as in the untreated control

[3] Unpublished data.

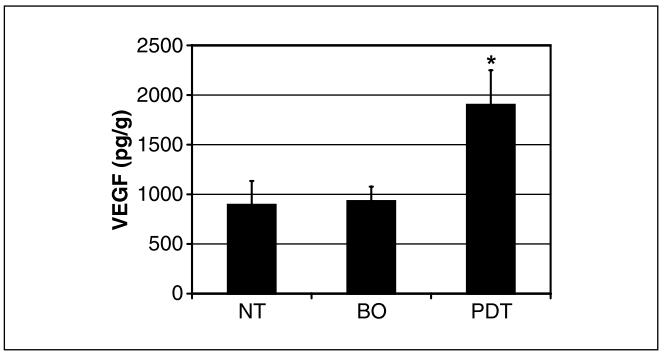

Figure 1. *In vivo* PDT increases VEGF. At 24 hours following treatment, orthotopic prostate tumors were collected, proteins were extracted, and VEGF levels were measured by ELISA. Values are normalized relative to protein concentration. *Columns,* mean of five animals for each group with each measurement done in duplicate; *bars,* SE. A statistically significant increase (*, $P < 0.05$) was measured following PDT when compared with no treatment or to BPD only. *NT,* no treatment; *BO,* BPD only.

animals (compare Fig. 2*A* with Fig. 2*C*), suggesting that the vasculature is less permeable.

Increased treatment efficacy when combining antiangiogenic therapy with PDT. It is well documented that VEGF is a potent angiogenic molecule (21, 22). Therefore, the measured increase in VEGF following PDT could reduce treatment efficacy by promoting tumor regrowth or potentially facilitating metastasis. For these reasons, we decided to investigate the efficacy of combining the antiangiogenic molecule, TNP-470, with PDT. Figure 3 shows the various groups used in this study. Group D received TNP-470 every 2 days the week preceding PDT, whereas group E received TNP-470 every 2 days for the week following PDT. All animals were sacrificed 40 days following orthotopic implantation and the prostate, composed of tumor tissue and normal tissue, was collected. The average weight loss and prostate volume for each group are shown in Table 1. The animals in all groups, except group E, had a weight loss of >3 g, whereas the weight of animals in group E did not change. Weight loss was measured by subtracting weight at sacrifice to weight at time of implantation. A statistically significant difference ($P < 0.05$) in weight loss between the groups receiving PDT + TNP-470 and the control, PDT alone, and the TNP-470 + PDT group could be measured. Prostate weight and prostate volume were also significantly reduced ($P < 0.05$) in the PDT + TNP-470 group when compared with the control group (Fig. 4*A*; Table 1). We did not measure any significant differences when TNP-470 was given before PDT. It is important to note that, in the current study, we used subcurative PDT doses; therefore, the tumors at day 40 are >400 mg compared with ~20 mg for normal prostate.

PDT increases the fraction of animals with lymph node metastases. At the time of sacrifice, the lungs, pelvic lymph nodes, liver, and spines were collected and metastatic spread was assessed. No metastases could be detected in the liver, spines, and lungs in all groups. On the other hand, lymph node metastases were detected in some animals of every group. Figure 5 shows a representative picture of a lymph node with a metastatic nodule. Sections were cut throughout the entire lymph node and stained with H&E and analyzed for metastases. Figure 4*B* shows the percentage of animals with lymph node metastases for each group. Similar to our previous report (8), more animals from group B (72%), which received only PDT, had metastases when compared with all other groups. Interestingly, the fraction of animals with lymph node metastases was reduced in all TNP-470-treated groups.

Discussion

PDT is an emerging modality for the treatment of various neoplastic and nonneoplastic pathologies. Because PDT is a dynamic process, the exact mechanism of tumor destruction and the accompanying molecular responses will depend on many factors, including the light and photosensitizer dose and the photosensitizer localization at the time of treatment. Depending on

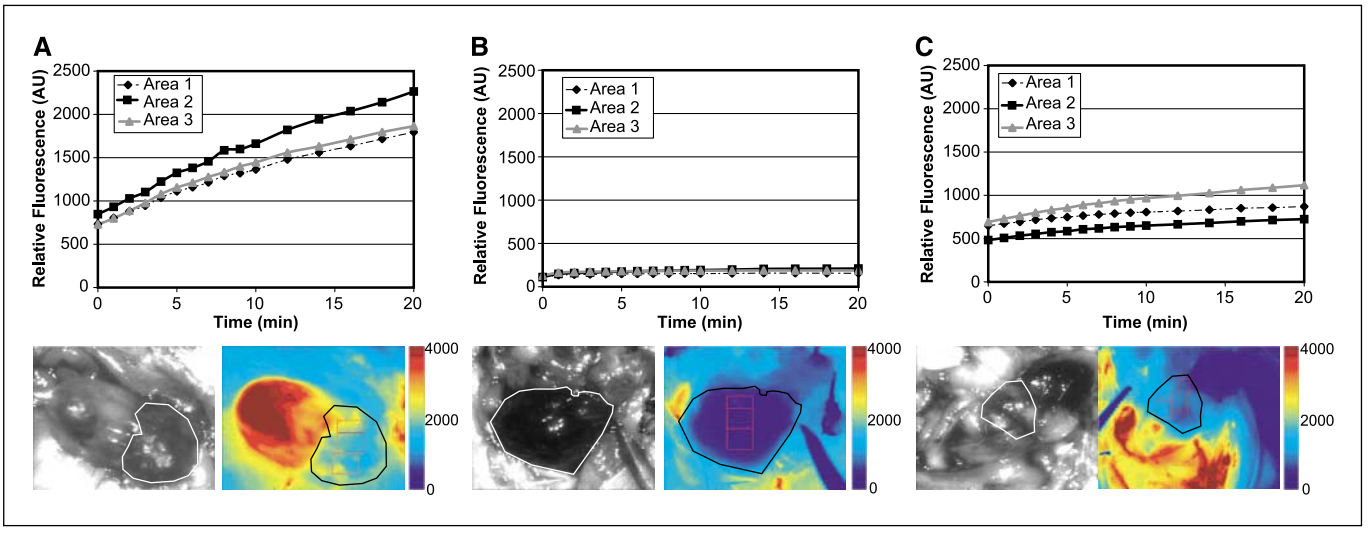

Figure 2. Analysis of tumor vasculature. The fluorescent molecule Alexa Fluor 647-BSA was injected i.v. immediately before imaging the prostate tumor with the Maestro *in vivo* imaging system. Diffusion of the fluorescent molecule was imaged every 1 minute for the first 10 minutes and every 2 minutes thereafter for a total imaging time of 20 minutes. *A* to *C, top,* relative fluorescence measurements in the tumor as a function of time. Data were acquired from each boxed area; *bottom,* representative black and white (*left*) or fluorescent pictures (*right*) from untreated animals (21 days following implantation, *A*), 24 hours after treatment (22 days following implantation, *B*), and 96 hours after treatment (24 days following implantation, *C*). Pictures were taken 20 minutes following fluorophore injection. *Line,* tumor borders; *box,* area used for fluorescence measurements. Representative pictures.

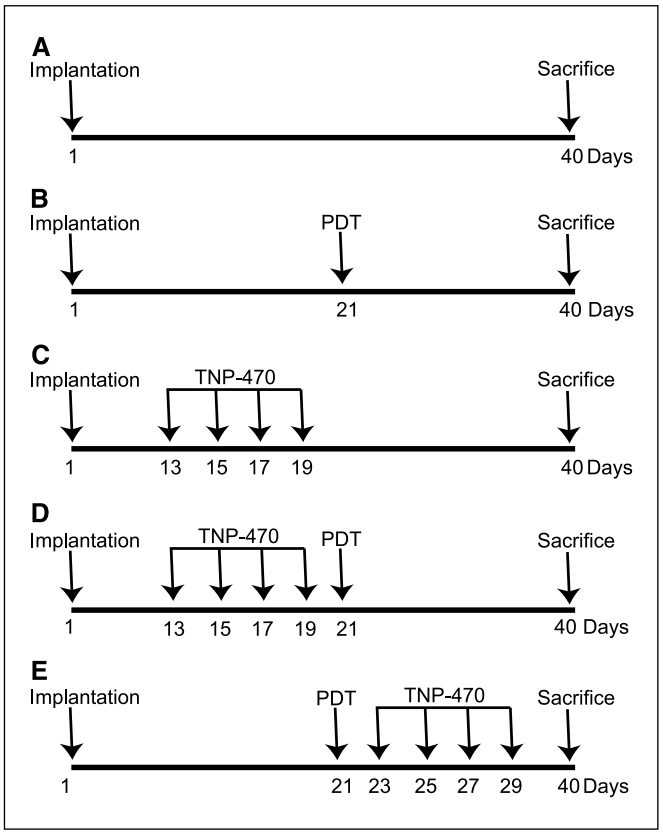

Figure 3. Treatment protocols. Orthotopic implantation of LNCaP cells in the prostate was done on day 1 and all animals were sacrificed on day 40. *A,* absolute control (n = 5). *B,* PDT alone (n = 7). *C,* TNP-470 alone (n = 5). *D,* TNP-470 treatment preceding PDT (n = 8). *E,* PDT followed by TNP-470 treatment (n = 5). TNP-470 was injected at 30 mg/kg body weight every 2 days for 1 week. PDT was done with 0.25 mg/kg liposomal BPD injected 1 hour before light irradiation (100 J/cm^2). n is the number of animals in each group.

the exact variables chosen, tumor destruction may be direct, from the induction of tumor cell apoptosis or necrosis (23), or indirect through vascular shutdown (24). The molecular responses of tumor cells to PDT may vary depending on the variables used and may mitigate PDT efficacy.

The feasibility of using PDT for the treatment of recurrent prostate cancer has been established previously (6, 7) and is now in early-phase clinical trials (5, 25). Due to the limited penetration depth of light in tissue and the nonhomogenous distribution of the photosensitizer in the tumor, some areas receive suboptimal PDT (either not enough light or not enough photosensitizer or both). Determining the molecular responses of these cells is therapeutically important as they may mitigate PDT efficacy. For example, an angiogenic response and an increase in metastases have been reported following subcurative PDT treatment (8, 12). Whether metastasis will be a problem in human studies is not clear at this point; however, the current study and previous studies (10, 12) suggest that subcurative PDT can create conditions favorable for tumor regrowth and metastasis. Using an orthotopic model of prostate cancer, we present here the first report of subcurative PDT-induced increase of VEGF secretion accompanied by an increase in the incidence of lymph node metastases. Importantly, the results show that, if the angiogenic action of VEGF is blocked by the antiangiogenic peptide, TNP-470, tumor growth, lymph node metastasis, and disease-related toxicity are all reduced.

As with our earlier study (9), all these experiments were done 1 hour after injection of liposomal BPD. Under this specific condition, the photosensitizer was localized both in the vasculature and intratumorally. The localization of the photosensitizer at the time of irradiation is a critical determinant of the mode of tumor destruction. In a recent study, Chen et al. showed that BPD-PDT 15 minutes after photosensitizer injection induced endothelial cell damage, causing vascular leakage, thrombi formation, and eventually, vascular shutdown (26). Hence, a vascular photosensitizer at the time of treatment will induce vascular shutdown, efficiently starving the tumor, whereas an intratumoral photosensitizer will cause tumor cell apoptosis or necrosis (27). Therefore, the current PDT treatment protocol could lead to both direct tumor destruction and indirect destruction through vascular shutdown. Consistent with this paradigm, *in vivo* animal imaging showed rapid vascular shutdown following PDT. However, 96 hours following treatment, functional vasculatures are present in the tumor (Fig. 2*C*). The measured VEGF increase following PDT could play a part in the formation of these new vessels. The PDT dose used in the present study was twice that reported previously (9) because it might be argued that a higher PDT dose could reduce VEGF induction by more effective destruction of tumor tissue or by the direct photochemical destruction of the VEGF protein. However, we were still able to measure an increase of VEGF 24 hours after PDT treatment. This suggests that, within the range of PDT doses used in the two studies, the VEGF increase is not strictly dependent on the light dose. At this point, it is not clear which PDT conditions might prevent the secretion of VEGF but systematic studies on this aspect are ongoing. We are also evaluating the direct contribution of VEGF on tumor regrowth and metastasis, using Avastin, a specific VEGF monoclonal antibody shown to inhibit its function (28).

An emerging concept in antiangiogenic therapy involves the 'normalization' of tumor vessels. Antiangiogenic therapies have been proposed as initially improving the structure and function of tumor vessels, resulting in an increase in tumor oxygenation. However, sustained treatment will eventually prune away tumor vessels, leading to hypoxia and, potentially, tumor destruction (for

Table 1. Treatment response

Groups	Weight loss (mean ± SE)	Prostate volume (mean ± SE)
A. Control (n = 5)	6.1 ± 0.5	761 ± 110
B. PDT (n = 7)	5.4 ± 0.5	407 ± 134
C. TNP-470 (n = 5)	3.1 ± 0.9	484 ± 94
D. TNP-470 + PDT (n = 8)	4 ± 0.4	696 ± 170
E. PDT + TNP-470 (n = 5)	−0.3 ± 0.9*	277 ± 116*

NOTE: Weight loss for animals (g) is calculated by subtracting weight at sacrifice to weight before injection. After sacrifice, prostate weight (normal tissue + tumor tissue) was determined (mg) and the prostate volume (mm^3) was measured. n is the number of animals in each group. For weight loss, there is a statistically significant difference (P < 0.05) between PDT + TNP-470 and control, PDT, and TNP-470 + PDT groups only. For prostate volume, there is a statistically significant difference (P < 0.05) only between PDT + TNP-470 and control.
*P < 0.05.

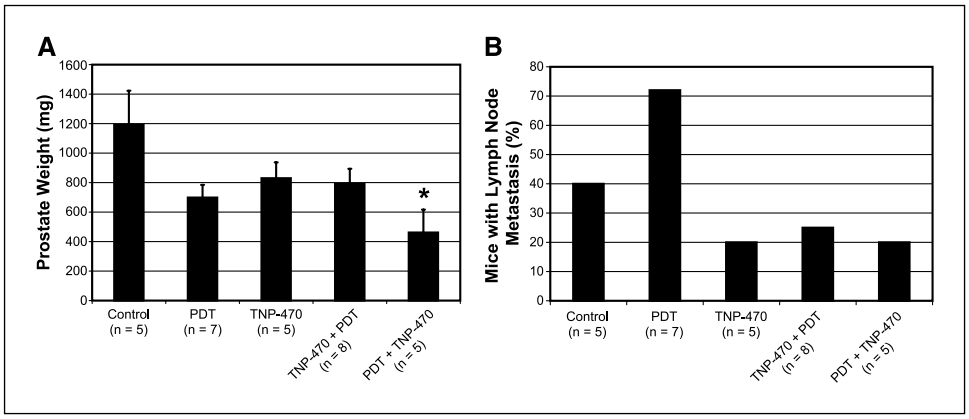

Figure 4. Combination treatment improves local tumor control and reduces metastases. *A,* animals from each group were euthanized 40 days following tumor cell implantation. The prostate, composed of both normal and tumor tissue, was weighed. There is a significant decrease (*, $P < 0.05$) in prostate weight in the PDT + TNP-470 group only when compared with the control. *B,* at the time of sacrifice, lymph nodes were collected, fixed in 10% formalin, and embedded in paraffin. Sections were cut throughout the lymph node and assessed for metastases. *n* is the number of animals in each group.

review, see ref. 29). Studies using TNP-470 and minocycline to treat s.c.-implanted gliosarcoma initially revealed a decrease in tumor hypoxia (30) and an increase in tumor oxygenation (31) compared with the untreated control. Similar observations were made with mouse mammary carcinomas (32). BPD-PDT is an oxygen-dependant treatment modality. Once activated, BPD transfers its energy to oxygen to generate the highly toxic singlet oxygen. Furthermore, numerous studies have correlated an increase in treatment efficacy with increased tumor oxygenation (33, 34). We therefore tested the effect of administering TNP-470 for 1 week before PDT (Fig. 3*D*). Compared with PDT alone, animals pretreated with TNP-470 tended to have a slightly higher prostate weight and prostate size (a measure of tumor burden). Although not significant, this difference could be due to the decrease in tumor vasculature, thereby limiting photosensitizer delivery. The best outcomes were obtained when TNP-470 was given after PDT (Fig. 3*E*) to inhibit the action of the PDT-induced angiogenic factors. This reduction of tumor burden is consistent with the hypothesis that TNP-470 interferes with the action of VEGF (or other angiogenic factors), thereby preventing tumor regrowth. It is also possible that PDT-treated cells become more susceptible to TNP-470 treatment.

Mechanistic studies have established that TNP-470 blocks MetAP2, an intracellular enzyme necessary for the process of protein myristoylation, thus preventing membrane proteins from being translocated to the cell surface (35). This causes inhibition of endothelial cell proliferation by inhibiting their cell cycle progression (17, 36–38). However, because protein myristoylation also occurs in other cell types, TNP-470 could have a direct effect on the proliferation of tumor cells (39). However, in our experiments, we did not observe a significant effect of TNP-470 treatment alone on prostate size and prostate weight when compared with the control group (Fig. 4*A*; Table 1). On the other hand, our results are consistent with the antiangiogenic action of TNP-470, although not necessarily demonstrative of antiangionesis.

LNCaP cells usually metastasize to the lymph node but can also metastasize to the lungs (40, 41). In a previous study, an increase in lung metastases following subcurative PDT in an orthotopic rat prostate cancer model was reported (8). In this study, we did not detect any lung metastases with the methods used in the study (Bouin's staining of perfused lungs). However, the presence of nodules not detectable by Bouin's solution is not ruled out. On the other hand, more animals in the PDT-treated group had an increase in lymph node metastases, suggesting that subcurative PDT generates conditions favorable to metastatic spread. Furthermore, the fraction of animals with lymph node metastases was reduced in all TNP-470-treated groups. This is consistent with the notion that the presence of the antiangiogenic molecule, TNP-470, could prevent the growth of colonized cells by inhibiting angiogenic support for the growing colonies or directly by preventing the release of cells from the tumor or both. Interestingly, when PDT treatment was curative, we did not observe any increase in metastases (8), suggesting that only surviving cells can elicit conditions favorable to spreading. Apparently, the subcurative outcome is due to the nonhomogenous distribution of the photosensitizer and/or of light in the tumor, suggesting that dosimetry measurements could improve treatment (42). The current study emphasizes the need for careful dosimetry to avoid partial responses that may have adverse long-term effects despite good local control.

In summary, this is the first report of inhibition of subcurative PDT-induced tumor growth and metastasis in an orthotopic model of cancer and suggests that the use of an angiogenic inhibitor, such as TNP-470 (which could also have a direct tumor cell growth-inhibitory effect), in combination with PDT could improve therapeutic outcomes in cancer patients and possibly reduce treatment-related toxicities from a given monotherapy. This study also suggests that a mechanism-based approach that directly inhibits VEGF secretion could enhance the therapeutic potential (43) of both PDT and antiangiogenic treatments and merits further investigations.

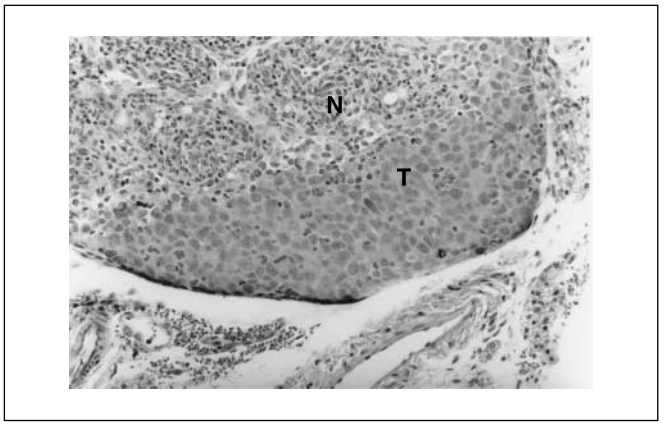

Figure 5. Metastatic nodule in lymph node. Representative picture of microsection from formalin-fixed lymph nodes that was stained with H&E. Metastatic spread was histologically determined. *T,* metastatic nodule; *N,* normal lymph node.

Acknowledgments

Received 5/16/2006; revised 9/1/2006; accepted 9/15/2006.

Grant support: NIH grants P01 CA84203 and RO1 EB00664 and Department of Defense grant PC040158 (N. Solban).

The costs of publication of this article were defrayed in part by the payment of page charges. This article must therefore be hereby marked *advertisement* in accordance with 18 U.S.C. Section 1734 solely to indicate this fact.

We thank QLT, Inc. for the gift of verteporfin/BPD, Dr. J. Folkman for TNP-470, Dr. W. Beecken for help with the animal model, and E. Davis for editorial help.

References

1. Solban N, Ortel B, Pogue B, Hasan T. Targeted optical imaging and photodynamic therapy. Ernst Schering Res Found Workshop 2005;49:229–58.
2. Brown SB, Brown EA, Walker I. The present and future role of photodynamic therapy in cancer treatment. Lancet Oncol 2004;5:497–508.
3. Hasan T, Ortel B, Solban N, Pogue B. Photodynamic therapy of cancer. 7th ed. In: Kufe, Bast, Hait, Hong, Pollock, Weichselbaum, et al., editors. Cancer medicine. Hamilton (Ontario): B.C. Decker, Inc.; 2006. p. 537–48.
4. Dougherty TJ. An update on photodynamic therapy applications. J Clin Laser Med Surg 2002;20:3–7.
5. Verigos K, Stripp DC, Mick R, et al. Updated results of a phase I trial of motexafin lutetium-mediated interstitial photodynamic therapy in patients with locally recurrent prostate cancer. J Environ Pathol Toxicol Oncol 2006;25:373–88.
6. Windahl T, Andersson SO, Lofgren L. Photodynamic therapy of localised prostatic cancer. Lancet 1990;336:1139.
7. Nathan TR, Whitelaw DE, Chang SC, et al. Photodynamic therapy for prostate cancer recurrence after radiotherapy: a phase I study. J Urol 2002;168:1427–32.
8. Momma T, Hamblin MR, Wu HC, Hasan T. Photodynamic therapy of orthotopic prostate cancer with benzoporphyrin derivative: local control and distant metastasis. Cancer Res 1998;58:5425–31.
9. Solban N, Selbo PK, Sinha AK, Chang SK, Hasan T. Mechanistic investigation and implications of PDT-induction of VEGF in prostate cancer. Cancer Res 2006; 66:1–8.
10. Ferrario A, von Tiehl KF, Rucker N, Schwarz MA, Gill PS, Gomer CJ. Antiangiogenic treatment enhances photodynamic therapy responsiveness in a mouse mammary carcinoma. Cancer Res 2000;60:4066–9.
11. Ferrario A, Von Tiehl K, Wong S, Luna M, Gomer CJ. Cyclooxygenase-2 inhibitor treatment enhances photodynamic therapy-mediated tumor response. Cancer Res 2002;62:3956–61.
12. Jiang F, Zhang ZG, Katakowski M, et al. Angiogenesis induced by photodynamic therapy in normal rat brains. Photochem Photobiol 2004;79:494–8.
13. Schmidt-Erfurth U, Schlotzer-Schrehard U, Cursiefen C, Michels S, Beckendorf A, Naumann GO. Influence of photodynamic therapy on expression of vascular endothelial growth factor (VEGF), VEGF receptor 3, and pigment epithelium-derived factor. Invest Ophthalmol Vis Sci 2003;44:4473–80.
14. Uehara H. Angiogenesis of prostate cancer and antiangiogenic therapy. J Med Invest 2003;50:146–53.
15. Adili F, Scholz T, Hille M, et al. Photodynamic therapy mediated induction of accelerated re-endothelialisation following injury to the arterial wall: implications for the prevention of postinterventional restenosis. Eur J Vasc Endovasc Surg 2002;24:166–75.
16. Du H, Bay BH, Mahendran R, Olivo M. Endogenous expression of interleukin-8 and interleukin-10 in nasopharyngeal carcinoma cells and the effect of photodynamic therapy. Int J Mol Med 2002;10:73–6.
17. Ingber D, Fujita T, Kishimoto S, et al. Synthetic analogues of fumagillin that inhibit angiogenesis and suppress tumour growth. Nature 1990;348:555–7.
18. Logothetis CJ, Wu KK, Finn LD, et al. Phase I trial of the angiogenesis inhibitor TNP-470 for progressive androgen-independent prostate cancer. Clin Cancer Res 2001;7:1198–203.
19. Retter AS, Figg WD, Dahut WL. The combination of antiangiogenic and cytotoxic agents in the treatment of prostate cancer. Clin Prostate Cancer 2003;2:153–9.
20. Figg WD, Kruger EA, Price DK, Kim S, Dahut WD. Inhibition of angiogenesis: treatment options for patients with metastatic prostate cancer. Invest New Drugs 2002;20:183–94.
21. Hrouda D, Nicol DL, Gardiner RA. The role of angiogenesis in prostate development and the pathogenesis of prostate cancer. Urol Res 2003;30:347–55.
22. Nicholson B, Theodorescu D. Angiogenesis and prostate cancer tumor growth. J Cell Biochem 2004;91: 125–50.
23. Ahmad N, Mukhtar H. Mechanism of photodynamic therapy-induced cell death. Methods Enzymol 2000;319: 342–58.
24. Wang HW, Putt ME, Emanuele MJ, et al. Treatment-induced changes in tumor oxygenation predict photodynamic therapy outcome. Cancer Res 2004;64:7553–61.
25. Weersink RA, Bogaards A, Gertner M, et al. Techniques for delivery and monitoring of TOOKAD (WST09)-mediated photodynamic therapy of the prostate: Clinical experience and practicalities. J Photochem Photobiol B 2005;79:211–22.
26. Chen B, Pogue BW, Luna JM, Hardman RL, Hoopes PJ, Hasan T. Tumor vascular permeabilization by vascular-targeting photosensitization: effects, mechanism, and therapeutic implications. Clin Cancer Res 2006;12:917–23.
27. Nowis D, Makowski M, Stoklosa T, Legat M, Issat T, Golab J. Direct tumor damage mechanisms of photodynamic therapy. Acta Biochim Pol 2005;52:339–52.
28. Ferrara N. Vascular endothelial growth factor: basic science and clinical progress. Endocr Rev 2004;25:581–611.
29. Jain RK. Normalization of tumor vasculature: an emerging concept in antiangiogenic therapy. Science 2005;307:58–62.
30. Teicher BA, Holden SA, Ara G, et al. Influence of an anti-angiogenic treatment on 9L gliosarcoma: oxygenation and response to cytotoxic therapy. Int J Cancer 1995;61:732–7.
31. Teicher BA, Dupuis NP, Emi Y, Ikebe M, Kakeji Y, Menon K. Increased efficacy of chemo- and radiotherapy by a hemoglobin solution in the 9L gliosarcoma. In Vivo 1995;9:11–8.
32. Teicher BA, Holden SA, Dupuis NP, et al. Potentiation of cytotoxic therapies by TNP-470 and minocycline in mice bearing EMT-6 mammary carcinoma. Breast Cancer Res Treat 1995;36:227–36.
33. Henderson BW, Gollnick SO, Snyder JW, et al. Choice of oxygen-conserving treatment regimen determines the inflammatory response and outcome of photodynamic therapy of tumors. Cancer Res 2004;64:2120–6.
34. Togashi H, Uehara M, Ikeda H, Inokuchi T. Fractionated photodynamic therapy for a human oral squamous cell carcinoma xenograft. Oral Oncol 2006;42:526–32.
35. Sin N, Meng L, Wang MQ, Wen JJ, Bornmann WG, Crews CM. The anti-angiogenic agent fumagillin covalently binds and inhibits the methionine aminopeptidase, MetAP-2. Proc Natl Acad Sci U S A 1997;94: 6099–103.
36. Yamamoto T, Sudo K, Fujita T. Significant inhibition of endothelial cell growth in tumor vasculature by an angiogenesis inhibitor, TNP-470 (AGM-1470). Anticancer Res 1994;14:1–3.
37. Zhang Y, Griffith EC, Sage J, Jacks T, Liu JO. Cell cycle inhibition by the anti-angiogenic agent TNP-470 is mediated by p53 and p21WAF1/CIP1. Proc Natl Acad Sci U S A 2000;97:6427–32.
38. Yeh JR, Mohan R, Crews CM. The antiangiogenic agent TNP-470 requires p53 and p21CIP/WAF for endothelial cell growth arrest. Proc Natl Acad Sci U S A 2000; 97:12782–7.
39. Sedlakova O, Sedlak J, Hunakova L, et al. Angiogenesis inhibitor TNP-470: cytotoxic effects on human neoplastic cell lines. Neoplasma 1999;46:283–9.
40. Wang X, An Z, Geller J, Hoffman RM. High-malignancy orthotopic nude mouse model of human prostate cancer LNCaP. Prostate 1999;39:182–6.
41. Sato N, Gleave ME, Bruchovsky N, Rennie PS, Beraldi E, Sullivan LD. A metastatic and androgen-sensitive human prostate cancer model using intraprostatic inoculation of LNCaP cells in SCID mice. Cancer Res 1997;57:1584–9.
42. Zhou X, Pogue BW, Chen B, et al. Pretreatment photosensitizer dosimetry reduces variation in tumor response. Int J Radiat Oncol Biol Phys 2006;64:1211–20.
43. Ferrario A, Gomer CJ. Avastin enhances photodynamic therapy treatment of Kaposi's sarcoma in a mouse tumor model. J Environ Pathol Toxicol Oncol 2006;25:251–60.

A Mechanism-Based Combination Therapy Reduces Local Tumor Growth and Metastasis in an Orthotopic Model of Prostate Cancer

Boleslav Kosharskyy, Nicolas Solban, Sung K. Chang, et al.

Cancer Res 2006;66:10953-10958.